Tanzania Journal of Science

Volume 51(3), 2025





Variations in extreme wet days during the OND rainy season in Tanzania and their linkages to atmospheric-oceanic anomalies

Philemon Henry^{1,2,3} and Paul TS Limbu^{4*}

¹State Key Laboratory of Climate System Prediction and Risk Management/Key Laboratory of Meteorological Disaster, Ministry of Education/Collaborative Innovation Center on Forecast and Evaluation of Meteorological Disasters, Nanjing University of Information Science and Technology, Nanjing, China.

²School of Atmospheric Sciences, Nanjing University of Information Science and Technology, Nanjing, China.

³Tanzania Meteorological Authority (TMA), Tanzania, University of Dodoma, Department of Computer Science and Intuitive Education, P.O. Box 27, 41218 Dodoma.

⁴Environmental and Atmospheric Sciences Group, Physics Department, University of Dar es Salaam, P. O. Box 35063, Dar es Salaam, Tanzania

Keywords

Extreme wettest days; OND; SST; Atmospheric circulation; Tanzania.

Abstract

Extreme rainfall remains one of the leading natural disasters in Tanzania, affecting the majority of citizens and the country's economy. Understanding the seasonal patterns and associated atmospheric and oceanic anomalies could help mitigate their impacts. The current study investigates changes in seasonal extreme wettest days (EWDs) rainfall in Tanzania and the associated atmospheric and oceanic anomalies during October-December (OND), from 1981 to 2020. EWD is defined as days when daily rainfall meets or exceeds the 99th percentile. Singular value decomposition (SVD), Mann-Kendall, t-test, and Pettitt test methods were applied in this study. The results indicate that approximately 2 EWD events were observed in many areas during OND, with fewer in central regions. Areas such as southwestern Lake Victoria Basin (LVB) and parts of the coastal regions experienced a significant increase in EWDs. The time series showed a non-significant positive trend, with a notable change in 2010. Generally, the country experienced an increase in EWD events in the recent decade. This increase is potentially associated with a shift in tropical SST from a cold phase to a warm phase, the incidence of low-level troughs over the tropical Indian Ocean (TIO), an increase in moisture flux convergence at the TIO, vertical velocity negative anomalies with the ascending limb of Walker-type circulation over the western Indian Ocean, and increased evaporation over the TIO and Congo basin. This is in line with the SVD results, which showed a strong coupling between EWDs in Tanzania and SST over the TIO, Pacific, and Atlantic Oceans, with significant correlation coefficients at the 99% confidence level of R=0.75, R=0.74, and R=0.76, respectively. This study provides valuable findings for farmers, forecasters and water users in Tanzania

Received 12 May 2024, Revised 20 May 2025, Accepted 30 May, Published October 30 2025 https://doi.org/10.65085/2507-7961.1047

© College of Natural and Applied Sciences, University of Dar es Salaam, 2025 ISSN 0856-1761, e-ISSN 2507-7961

^{*}Corresponding Email: paul.limbu@ymail.com

Introduction

Rainfall remains a crucial weather variable that significantly affects human society and natural ecosystems (Conway 2002, Han et al. 2021). In recent decades, there have been significant changes in its temporal and spatial patterns, including an increase in extreme rainfall events globally (IPCC 2012, WMO 2023). These changes contribute to unpredictable floods and longerlasting droughts, both of which have a significant adverse impact on countries such as Tanzania (the study area), where 75% of the population relies heavily on rain-fed agriculture activities (Thornton et al. 2014, USAID 2018). In Tanzania, rainfall is primarily influenced by the Intertropical Convergence Zone (ITCZ), resulting in a bimodal rainfall pattern with two wet seasons: March-May (MAM) and October-December, OND (Black et al. 2003, Kijazi and Reason 2011). The frequency, timing and intensity of rainfall during these seasons vary due to several factors such as topographic features, atmospheric systems and the position of the ITCZ (Palmer et al. 2023). The ITCZ typically moves northward during MAM, which is associated with more rains, and returns south across the equator during OND, bringing more rains in November and December, particularly over the northern, northeastern and eastern coast regions (Nairobi 1979, Borhara et al. 2020). The rainfall distribution of a country is well demonstrated by the number of rain days rather than monthly, seasonal or annual rainfall accumulation (Nandargi and Mulye 2012). These rainfall days provide necessary information that can be used to mitigate rainfall-related disasters (Han et al. 2021). Excessive or insufficient rain days within a season may likely instigate floods, droughts and the emergence of crop insects (such as aphids and leafhoppers) and human diseases (such as Rift Valley fever and dengue), which may significantly impact various economic sectors such as agriculture and health (Tadross et al. 2009, Anyamba et al. 2014, Kotz et al. 2022). Addressing extreme wettest days (EWDs) is a key step in poverty reduction in countries such as Tanzania, since the majority of citizens heavily depend on rain-fed agriculture, which is affected mostly by extreme rainfall events (Chang'a et al. 2020, Wainwright et al. 2020).

Seasonal rainfall in East Africa (EA) has shown high variation, with an increase in extreme events (Lyon and DeWitt 2012, Owiti 2012), instigated by local and global factors, such as the Congo Basin air mass, which serves as a moisture source for rainfall in Tanzania (Mugalavai et al. 2008, Ntwali et al. 2016, Spracklen et al. 2012). Tropical Cyclones in the southwestern Indian Ocean (SWIO), EA monsoons, and variation of sea surface temperatures (SSTs) over the tropical Indian Ocean (TIO), both of which modify atmospheric patterns over the region that modulate rainfall (Kilavi et al. 2018, Finney et al. 2019, Kebacho 2022b). Other drivers, such as variation of SSTs over the North and South Atlantic Ocean, El Niño Southern Oscillation (ENSO) and Indian Ocean Dipole (IOD), are also strongly linked with rainfall in EA (Ashok et al. 2001, Saji and Yamagata 2003, Wagesho and Claire 2016, Limbu and Guirong 2020). Additionally, the eastward propagation of the Madden-Julian Oscillation and the eastward phase of the Quasi-Biennial Oscillation also control rainfall over EA (Indeje and Semazzi 2000, Vellinga and Milton 2018).

The oceanic phenomena like positive IOD (pIOD) and El Niño significantly enhance atmospheric moisture in EA, leading to extreme rainfall events, particularly during OND and December to February (Black et al. 2003, Saji and Yamagata 2003, Chang'a et al. 2020, Wainwright et al. 2020). Years with simultaneously positive IOD and El Niño are associated with above-normal rainfall over most areas in EA (Rwambo et al. 2025). The pIOD phase leads to substantial rains in the central and southern highlands of Tanzania, while El Niño significantly impact coastal areas during December-February, impacts are more substantial when both phenomena coincide (Wenhaji et al. 2018, Mbigi and Xiao 2021). Rising SST in the TIO and convective activity in the western Indian Ocean (WIO) modulate moisture flow to some regions in Tanzania during OND

(Kijazi and Reason 2009). However, other studies (e.g., Wainwright et al. 2020, Kebacho 2022a; Semgomba et al. 2025) discovered that Equatorial EA experiences wet years when TC is located over southern Madagascar, which draws air from higher latitudes, enhancing southerly wind flow and also pulling westerly winds to the adjacent Indian Ocean across the Mozambique Channel. Additionally, EA also witnesses westerly moisture winds across Lake Victoria during phases 3 and 4 of the MJO, modulating heavy rainfall during MAM and OND (Finney et al. 2019, Wainwright et al. 2020).

The frequency, intensity and duration of extreme rainfall events in EA, particularly in Tanzania, vary from season to season (Ongoma et al. 2016, Ojara et al. 2021). The studies conducted by Japheth et al. (2021) and Mtewele et al. (2021) revealed an increase in the frequency and intensity of heavy rainfall events between January and May over the northern sector and the coast zone of Tanzania. Also, a recent study conducted by Ndabagenga et al. (2023) revealed an annual increase in extreme rainfall events in Tanzania between 1981 and 2020. Generally, the majority of previous studies conducted in EA demonstrate that extreme rainfall events are increasing in some areas, despite some studies, such as Lyon and DeWitt. (2012) as well as Makula and Zhou. (2021), indicated a decrease of extreme rainfall events in seasonal rainfall. This is the reason motivating the authors to explore changes in seasonal EWDs rainfall in Tanzania and the response of the atmospheric circulation and oceanic anomalies. This topic

has received less attention in EA since most of the previous studies focused only on extreme rainfall in terms of rainfall amount. This study fills the gap by seeking answers to the following questions: How frequently have EWDs been reported in Tanzania during OND for the period 1981–2020? Is the trend in EWD occurrence during the OND season from 1981 to 2020 statistically significant? Have there been any changes in the patterns of EWDs between 1981 and 2020, and how do atmospheric and oceanic anomalies respond to these changes? Lastly, to what extent are the SSTs in the TIO, Pacific Ocean and Atlantic Ocean related to the EWD variations over Tanzania during OND?

Data and Methodology Study domain

Tanzania is a country in eastern Africa (Figure 1), which is bordered by Kenya and Uganda to the north, Rwanda, Burundi and the Democratic Republic of the Congo to the west, Zambia and Malawi to the southwest, and Mozambique to the south. However, the country is surrounded by larger water bodies such as the Indian Ocean, Lake Victoria, Lake Tanganyika and Lake Nyasa. Lake Victoria is the largest lake in Africa and the second largest freshwater lake in the world, while Lake Tanganyika is the second deepest in Africa and the deepest in EA (Verburg and Hecky 2009, Awange et al. 2019, Nyamweya et al. 2023). The presence of the highest mountains, such as Mount Kilimanjaro and other geographical features contributes to local weather and seasonal rainfall (Ogwang et al. 2012).

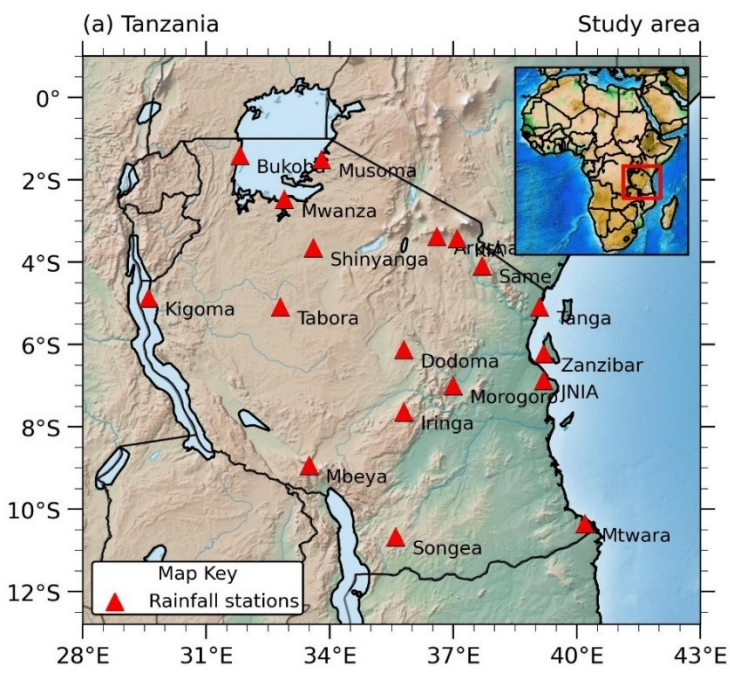


Figure 1: The study domain (Tanzania). The red box at the top right corner of the figure indicates the location of the study area on the Africa map.

Data

This study used daily ground observation data from 18 synoptic agrometeorological stations (Figure 1) from 1981 to 2020. The study also utilised daily gridded rainfall data from Climate Hazards Group InfraRed Precipitation with Station data (CHIRPS v2.0), which has a resolution of 0.05° x 0.05° (Funk et al. 2014, 2015), which is widely used in the meteorological field in the EA region previously studies (e.g., Dinku et al. 2018, Ojara et al. 2021, Yonah et al. 2023, Omay et al. 2023). CHIRPS data were combined with rainfall from 18 observation stations, using a similar technique applied by the International Research Institute for Climate and Society to generate Enhancing National Climate Services (ENACTS) data in Africa and Asia (Acharva et al. 2020, Dinku et al. 2022). This process improves the quality and strengthens the robustness of the extracted EWD. The station data quality assessments and data merging process were conducted by using Climate Data Tools (CDT) in R (Dinku et al. 2022).

The present study also utilised monthly mean reanalysis data to identify changes in circulation atmospheric Atmospheric parameters such as specific humidity, zonal and meridional winds and geopotential height were obtained from NCEP/NCAR Reanalysis 1 and covered 40 years from 1981 to 2020, with a resolution of 2.5° x 2.5° (Kalnay et al. 1996). The specific humidity, zonal and meridional winds were used to compute the vertically integrated moisture flux (VIMF) and convergence (VIMFC). Furthermore, global monthly mean COBE-SST data obtained from the NOAA with a resolution of 1.0° x 1.0°, spanning from 1981 to 2020 (Ishii et al., 2005), were used to investigate changes in SST anomalies and the linkage between SSTs over the tropical Indian, Pacific, and Atlantic Oceans **EWDs** and over Tanzania. Monthly evaporation data from the European Centre Medium-Range Weather Forecasts (ECMWF), fifth generation with a resolution of 0.25° x 0.25° and timespan from 1981 to 2020 (Hastenrath 2007, Hersbach et al. 2020), were also used to exhibit the change of

evaporation anomalies. However, it is better to know that the negative evaporation values in ERA5 represent evaporation, while positive values for condensation.

Methodologies Definition of extreme wettest rain days

The present study used a percentile-based approach to compute EWDs. EWD is defined as days where daily rainfall meets or exceeds the 99th percentile, calculated from the distribution of all rainy days (daily rainfall >1.0 mm) at each grid cell during the OND seasons from 1981 to 2020, as used in Li and Wang (2018) and Mastrantonas et al. (2020). This criterion is applied only to select grids with sufficient rainfall data for analysis of EWDs. The number of EWDs is determined by the count of rainy days exceeding the 99th percentile threshold. The 99th percentile thresholds for daily rainfall vary spatially across the study area and temporally within the seasons (Gamoyo et al., 2014). The range of these thresholds highlights the spatial and seasonal variability in extreme rainfall conditions. The applied approach is similar to R99p index, one of the 27 climate indices recommended by the World Meteorological Organisation (WMO).

Spatiotemporal analysis of EWDs trend

The present study utilises a linear regression to show the temporal trend of EWDs in each rainfall season. This method has been used in previous studies by Wang et al. (2012) and (2017), to investigate trends of the temperature and precipitation extreme events over Xinjiang, northwestern China. The significance of the obtained trend was then tested by the Mann-Kendall (MK) trend test approach, whereby the significance of trends was demonstrated by the p-value technique (p-value ≤ 0.05 as 95% confidence level and 0.1 as 90% confidence level). This method is based on normally distributed data and has a low sensitivity to abrupt changes in homogeneity data series (Mann 1945, Kendall 1975). The study also applied MK to look for the spatial trend of EWDs from each grid cell. The p-value ≤ 0.05 from this method was used to display areas

characterised by significant increases or decreases trend at the 95% confidence level.

Analysis of trend change detection, occurrence and anomalies

The Pettitt test method was applied to detect the sensitivity of abrupt changes of the trend in a series of EWD data from 1981 to 2020. Pettitt is a non-parametric statistical test useful for detecting abrupt changes in the mean of the data series and provides a single point as a trend change reference (Pettitt 1979, Xie et al. 2014). The method revealed a point before the change (first period) and after the change (second period). Therefore, in this study years before the changes (1981-2009) and after the changes (2010-2020) further identified for analysis. were Anomalies were also applied to explore atmospheric circulations under selected periods. The climatology mean from 1991 to 2020 was considered as the base period for anomaly computation. The student *t*-test was also deployed between two selected periods to reveal significant patterns associated with changes. The Probability Density Function (PDF) was also applied to illustrate the occurrence and changes of EWDs, which is typically used to display the amplitude and distribution of EWDs within periods. A similar technique was applied previously in studies of Alexander et al. (2006) and Wang et al. (2012) to investigate changes in extreme rainfall events in China.

Analysis of the moisture transportation

Vertically integrated moisture (VIMF) was analysed to reveal patterns of horizontal moisture transportation through the troposphere in the first and second periods, and their differences. VIMF is closely related to rainfall variation at the surface and defined as the amount of water vapour absorbed or radiated per unit time and volume (Li et al. 2013, Ma et al. 2022). VIMF was integrated from 1000 hPa to 300 hPa by ignoring levels above 300 hPa due to specific humidity. This technique includes multiple layers and overcomes obstacles such as larger terrain at lower levels (Fasullo and Webster 2003, Ma et al. 2022). The study also applied a partial derivative to the VIMF to achieve vertically integrated

moisture flux convergence (VIMFC), identifying areas with water vapour convergence (Chansaengkrachang et al. 2018). Mathematically, VIMF is illustrated in Equation 1, and VIMFC is presented in Equation 2.

$$VIMF = \frac{1}{g} \left(\int_{300}^{1000} qu \, dl p + \int_{300}^{1000} qv \, dl p \right)$$
 (1)

$$VINFC = \frac{-1}{g} \left(\frac{\partial \left(\int_{300}^{1000} qu \, dl p \right)}{\partial x} + \frac{\partial \left(\int_{300}^{1000} qv \, dl p \right)}{\partial y} \right)$$
(2)

where: g stands for gravitational acceleration ($g \cong 9.81 \, ms^{-2}$), q is specific humidity (kg/kg), u represents zonal (longitude) wind (ms^{-1}), and v represents meridional (latitude) wind (ms^{-1}). dp (hPa) represent layer thickness along the pressure levels. Also, ∂x and ∂y stand for grid spaces along the east-west and north-south directions, respectively.

Analysis of coupled patterns between EWDs and SST anomalies

The singular value decomposition (SVD) method was utilised to explore coupled patterns between EWDs over Tanzania and SSTs over the TIO, Pacific and Atlantic Oceans during the first and second periods. The method decomposes the covariance matrix of two fields into singular values and creates two sets of paired-orthogonal vectors, known as loading maps, representing spatial patterns. The method generates the squared covariance fraction (SCF), which is a crucial metric for assessing the significance of different modes in the decomposition (Prohaska 1976). The advantage of this method, reveals areas with similar patterns. The method has been applied in several studies in Tanzania (e.g., Mafuru and Guirong 2020, Limbu and Guirong 2020, Makula et al. 2020).

Results and Discussion Spatiotemporal distribution, occurrence and trends of the EWDs

The result of seasonal mean EWDs during OND (Figure 2a) reveals that most parts of the country experience 1 to 2 EWDs, with no events in the central parts and some areas around LVB. These areas may benefit from moisture originating from the Congo basin and surrounding water bodies, primarily due to their contribution to abundant moisture availability, which can enhance rainfall patterns, as suggested in (Dinku et al. 2010). The study highlights the influence of large water bodies, such as the Indian Ocean, in modulating local rainfall due to their ability to provide moisture to the atmosphere. As shown in Figure 2b, the seasonal EWD patterns during OND over the coastal belt and western regions are consistent with the climatological observed rainfall presented in (Gamoyo et al. 2014). This result does not exhibit systematic overestimation or underestimation. Aligning with the unbiased seasonal rainfall at the 99th percentile (Figure 2c), which demonstrates the apparent balance in seasonal rainfall, is therefore not due to compensatory seasonal biases but rather reflects the inherent accuracy of the seasonal EWD climatology as derived from the These results underscore reliability of the methodology and suggest that the observed seasonal EWD patterns accurately represent regional climatic behaviour. The MK results in OND (Figure 2b) show a non-significant decrease in EWDs regions. over most except for southwestern parts of the LVB, where EWDs significantly increase at a 95% confidence level.

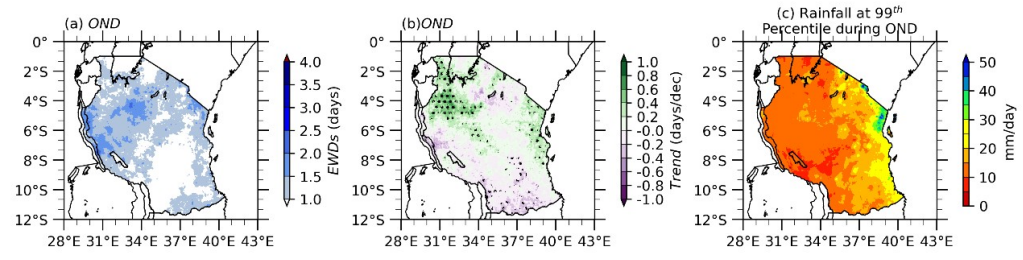


Figure 2: Spatial patterns of the (a) mean EWDs, (b) EWD trend during 1981-2020 and (c) Rainfall threshold at 99^{th} percentile during OND. The stippling indicates a significant area with the 95% confidence level when the p-value ≤ 0.05 .

The analysis of MK (Figure 3a) shows a non-significant positive trend with high EWDs in 1997 and 2019, and lowest in 1993 and 2005. The season (OND) experienced a non-significant abrupt change in 2010 according to Pettitt test result, suggesting a slight upward shift in EWD, starting from 2010 to 2020. Most of the years between 1981 and 2009 experienced relatively fewer EWDs, with a high peak in 1997. It is important to note that the detected change around 2010 indicates potential characteristics of EWDs between periods, as indicated in Table 1. The average values of EWDs during two distinct periods, before and after the change, show a slight increase from 0.96 to 1.24 days. The Pettitt test suggests that any changes in the temporal distribution of EWDs are less pronounced and not-significant. This could imply that OND rainfall extremes are more influenced by inter-annual variability rather than possibly related to large-scale phenomena such as the IOD or ENSO (Wainwright et al. 2020), generally associated with extreme rainfall events. Therefore, these events are likely to be among the factors influencing EWDs in Tanzania. This motivates us to investigate further how SSTs are related to EWDs between periods by using SVD technique.

Table 1: Summary results of the Pettitt test for the abrupt trend change in EWDs.

Season	Change- point	1 st period	2 nd period	Mean of the 1 st period	Mean of the 2 nd period	P-value
OND	2010	1981-2009	2010-2020	0.96	1.24	0.491

Note: p-value with * is statistically significant at the 90% confidence level.

Figure 3(b) explains the distribution of EWDs in Tanzania during the OND seasons which shows a slightly higher maximum PDF value of 0.76, with an average occurrence of around 1 EWD. This reflects a higher chance of isolated EWDs in this season. The vertical dashed red lines, representing the 95th percentile of EWD occurrences, further support these observations, which reflect a lower frequency of EWDs, consistent with the shorter and more irregular nature of

EWDs during this period. Additionally, the tails of the PDF curves offer insights into the distribution of EWDs. The broader tail and skewed PDF peak points out higher concentration of the EWDs in shorter periods, with stronger variability of wet conditions. These findings underscore the seasonal variability in EWD patterns in Tanzania, with a higher probability of isolated EWDs occurring over shorter durations.

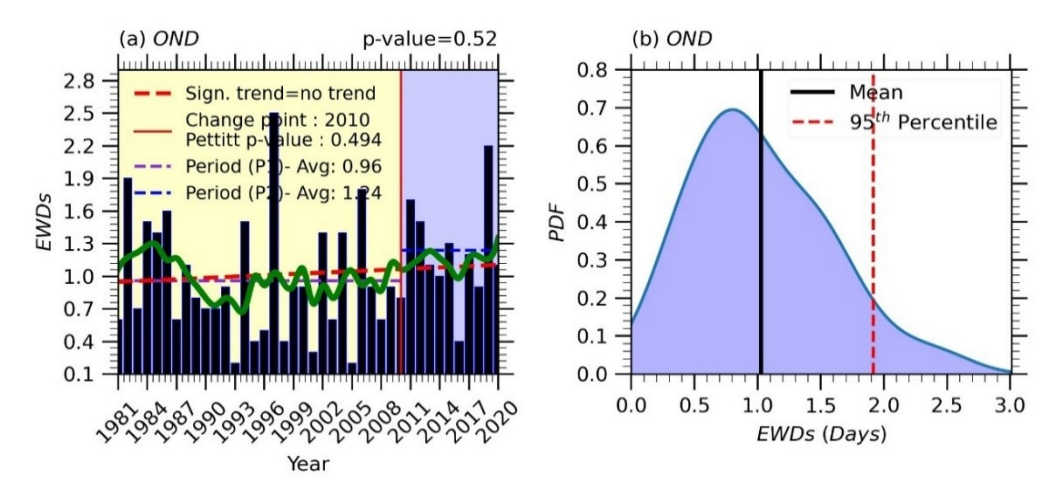


Figure 3: Temporal patterns of bar graph and Probability Distribution Function (PDF) of EWDs during OND computed based on the country area averaged. (a) Bar-graph of EWD and (b) PDF of EWDs.

The solid vertical black line in PDF indicates the mean value, while the dashed vertical red line indicates the 95th percentile of the distributed EWDs. A shaded light yellow at the back of bar graphs shows years with EWDs before updraft change (first period), while a light blue indicates years after updraft change (second period), which are separated by the red line. The solid green line in the bar graph indicates the 6-year running average.

Change and trend of the seasonal EWDs

The changes and trends in EWDs based on the selected periods presented in Table 1 and their differences, were obtained by subtracting the second period from the first period. The results in Figure 4(a) show a significant decrease in trend from 1981 to 2009 during the first period over southern and

western areas. Moreover, the second period from 2010 to 2020 (Figure 4b) shows nonsignificant positive trend patterns in the western LVB and along the eastern coast belt, with a significant decrease in central regions, extending to SWH. The difference between periods (Figure 4c) shows that EWD patterns become stronger in the northwest of the LVB and weaken in the rest of the area, particularly in southern regions. This is in line with the results of (Ndabagenga et al. 2023), which studied the extreme rainfall in Tanzania. Overall, the findings indicate a significant positive shift in EWDs with a positive trend, particularly in bimodal areas where ITCZ and factors such as El Niño and positive IOD are linked to rains during this season.

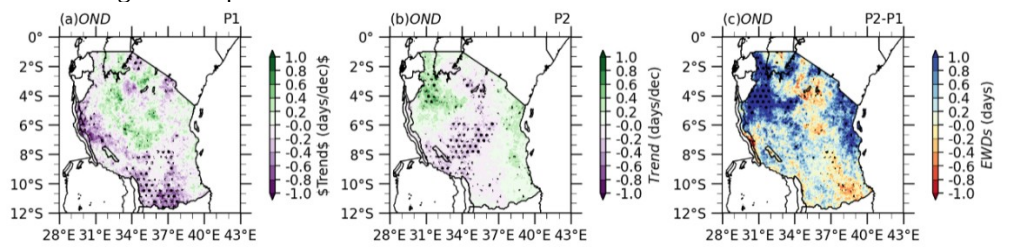


Figure 4: Trend patterns in the first (a) and second periods (b) with their corresponding differences (c) in EWDs during OND. The stippling from plots (a) to (b) indicate a significant trend when the p-value ≤ 0.05 , and those in plot (c) show significant change at the 95% confidence level of the difference between periods based on the Student *t*-test.

Figure 5 displays the PDFs of EWDs during the first and second periods, along with their changes based on their averages presented in solid black and blue lines. The concept was also used previously in the studies of Wang et al. (2012) and Alexander et al. (2006). The results indicate that the vears between 2010 and 2020 in the second experienced relatively period а frequency of PDF with the same number of EWDs between periods, indicating a high chance of occurring EWDs in the second period. Generally, the shifting of the vertical mean line in the second period to the right of the first period explicitly shows a recent increase in EWD events in Tanzania, the same as that indicated in Figure 3(a). However, the change between periods demonstrates less magnitude but usually may result in a devastating impact on the environment and society. Furthermore, the similarity of extended right tails between periods demonstrates less variability and no substantial change in the number of EWD in Tanzania.

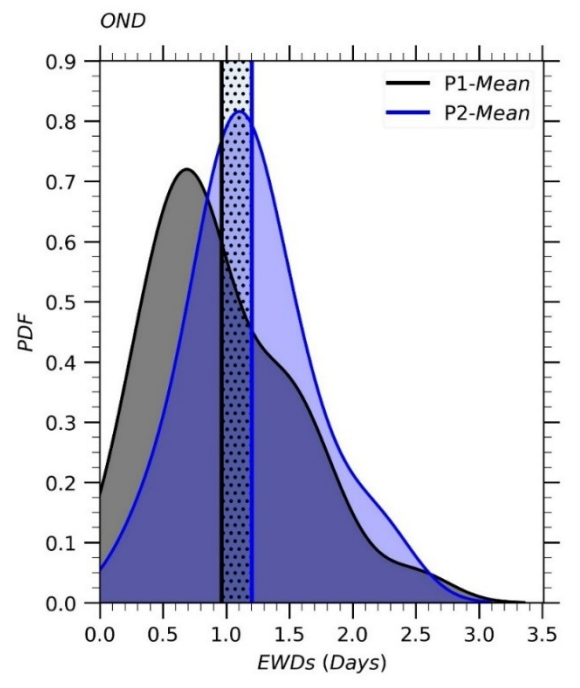


Figure 5: The Probability Distribution Function of EWDs during the first period (shaded in dark grey) and second period (shaded in light blue). The black vertical solid line stands for an average of EWDs in the first period (denoted as P1-mean), and the blue solid line stands for an average of EWDs in the second period (denoted as P2-mean). The dots in between vertical black and blue lines indicate a change in the mean EWDs between periods.

Changes in atmospheric circulations and SST anomalies

Moisture transportations and their linear relationship to EWDs

Moisture transportation is closely linked to surface rainfall (Ma et al. 2022). The VIMF from 1000 to 300 hPa and convergence results show potential areas characterised by moisture flux and

convergence anomalies in the first and second period during OND, along with their differences. The study reveals that water vapour is transported from the SWIO to Tanzania from 1981 to 2009 during the first period and from 2010 to 2020 in the second period (Figure 6a and b), with divergence in the western part of the domain. The difference between VIMF vectors between

periods (Figure 6c) shows that moisture is transported from the west with intense vectors, while convergence is increasing over most parts of the country except for the southern region. The result also shows that the country is characterised by southeasterly to easterly VIMF vectors during this season, supporting findings presented in (Zhang et al. 2015). Generally, moisture convergence dominates over the central to eastern part of the domain and in the TIO, while divergence

is seen in the western part of the domain. The difference between periods reveals westerly moisture flux vectors across the Congo Basin towards Tanzania, which mostly enhance rainfall in the domain. Similar results were also presented in Clark et al. (2003) and Ntwali et al. (2016), demonstrating that westerly moist winds from the Congo Basin typically influence rainfall in EA.

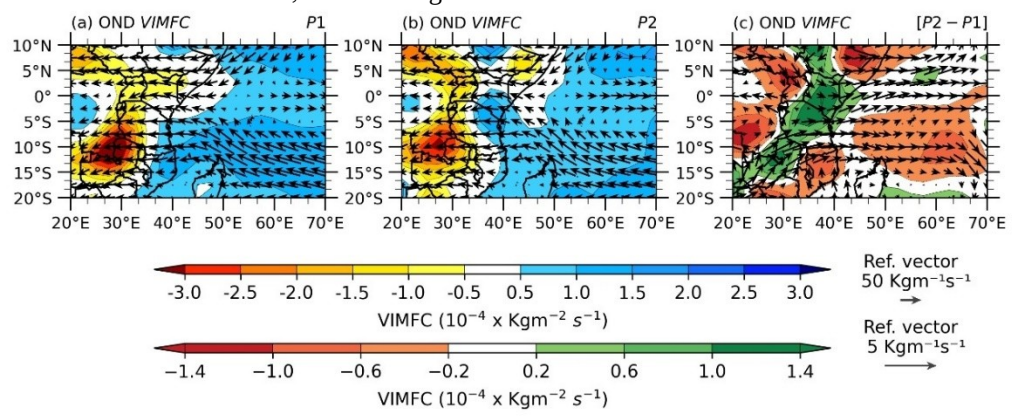


Figure 6: Vertical integrated moisture flux (VIMF) convergence (VIMFC) anomalies during OND (unit: 10^{-4} x kg m^{-2} s⁻¹ for the VIMFC, while unit: kg m^{-1} s⁻¹ stands for VIMF vectors). The results were integrated from 1000 hPa to 300 hPa for the first (a), second periods (b) and their corresponding differences (c). The shaded positive (negative) values represent moisture convergence (divergence).

The VIMFC anomaly observed over the TIO in Figure (6) motivates the present study to investigate whether there is an existing connection between the VIMFC anomaly over the Indian Ocean and EWDs in VIMFC Tanzania. The anomaly (only positive anomalies) was computed by area averaged over the region bounded between (40°-70° E and 20° S-10° N). The same technique previously was (Chansaengkrachang et al. 2018). The results are presented in a scatter plot with a correlation coefficient (R). The results show that more patterns are concentrated between 0.6 and 1.1 EWDs, and 0.0 and 0.4 x 10^{-2} VIMFC index in the first period (Figure 6a), while more patterns are scattered in the second period (Figure 6b). Further results from Figure 6(a) reveal a positive relationship between the VIMFC index and

during OND. The relationship significantly increased in the second period. where $R \cong 0.65$. Additionally, results also reveal days with both low (high) moisture convergence and EWDs, at the lower left (upper right) corner in Figure 6(a and b), suggest days with minimum (maximum) atmospheric moisture inflow, consequently less (heavy) rainfall. Such conditions might be typical of dry (wet) or stable (unstable) atmospheric conditions. Moreover, patterns in the lower (upper) right (left) corner, characterised by low (high) VIMFC and high (low) EWDs, suggest days with low (high) moisture convergence but high precipitation. These conditions could occur when local factors, such as convection or localised topographic effects, lead to heavy (less) rainfall despite low (high) column total moisture convergence.

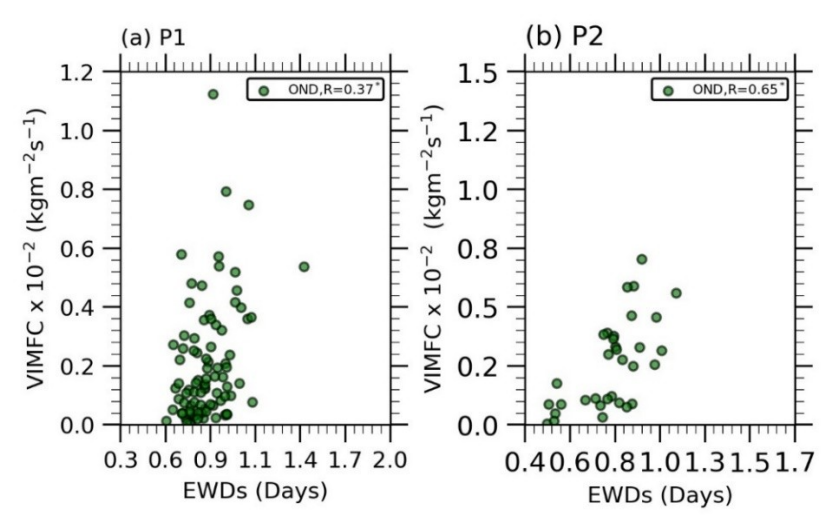


Figure 7: Relationship between vertical integrated moisture flux convergence (VIMFC) index anomalies (only positive values) and EWDs during OND in the first period (a) and second period (b). The VIMFC index was computed based on the area averaged over the TIO between 40°-70° E and 20° S-10° N. The correlation values with the star (*) are significant at the 95% confidence level based on the Student *t*-test.

Atmospheric circulation anomalies

The changes in evaporation, geopotential height (GPH), vertical velocity and wind (zonal and meridional) during periods, and their differences were also examined. For instance, evaporation influences the overall moisture content in the atmosphere, with other factors playing a role in modulating rainfall. The results (Figure 7a) show that during the first period, there is a decrease in evaporation (positive anomalies based on ERA5 document) over the tropical WIO and Congo basin, while the remaining areas are characterised by a slight increase evaporation (negative anomalies based on ERA5 document). The strong patterns of evaporation shift to the northern part of the Indian Ocean, over the coast regions and LVB. The difference between periods (Figure increase significant 7c) shows a evaporation over the northern and coastal areas. This increase in evaporation is likely due to the warming of tropical Indian SST anomalies, as shown in Figure 9, which is considered to be among the drivers behind the recent increase in EWDs in Tanzania.

Further analysis shows that most areas of the target domain (Tanzania) experienced negative GPH anomalies, justifying the presence of a trough at low-level in the first period (Figure 7d), with positive anomalies across parts of TIO, suggesting the presence of a ridge. In the second period (Figure 7e), the patterns shifted to positive anomalies over the target domain and negative across TIO, demonstrating that the influence of TIO SST on convergence activities is predominant during this period. The difference between periods shows an increase in GPH anomalies across Tanzania, with the significant negative GPH anomalies over SWIO and northern parts, which contribute to westerly moisture winds inflow toward Tanzania as indicated in Figure 6(c), which usually enhances rainfall. The upper troposphere at 200 hPa (the figure is not included) generally reveals negative (positive) GPH anomalies in the first (second) period, which allows upper-level convergence (divergence) over the domain (TIO). Additionally, significant patterns at the 95% confidence level of negative anomalies in Figure 7(c) suggest that

increasing upper GPH anomalies may enhance surface convergence that modulates

rainfall, aligning with findings of Wiston and Mphale (2019).

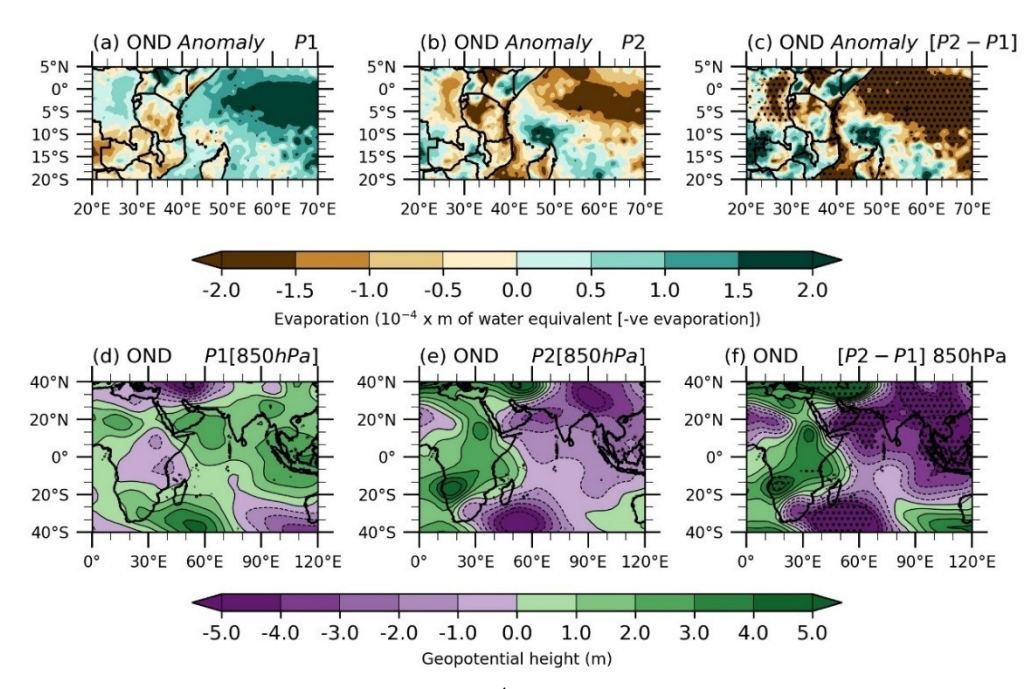


Figure 8: Evaporation anomalies (unit: $10^{-4} \chi m$ of water equivalent), during the first period (a) and second period (b) with their corresponding differences (c). Geopotential height anomalies (unit: m) at the low-level troposphere (850hPa) during the first period, second period, and their corresponding differences are also presented in (d), (e) and (f), respectively. Stippling indicates a significant area at a 95% confidence level based on the Student *t*-test.

The analysis of the vertical cross-section of the vertical velocity and zonal wind was also conducted to explore the atmospheric stability. Results show that during the first period (Figure 8a), areas over the tropical eastern (western) Indian Ocean experience descending (ascending) motion downward (upward) wind vectors, lessening (enhancing) rainfall formation over the target domain. In the second period (Figure 8b), there is ascending motion with upward wind and negative vertical velocity anomalies over Tanzania and eastern Indian Ocean, supporting convective activities over the targeted domain (left side of the black dotted line). Additionally, the WIO is characterised by a well-defined Walker-type circulation with rising air near our area of interest and sinking air in the central Indian Ocean, especially in the second period. These patterns intensify significantly at a 95% confidence level when the first period is subtracted from the second period (Figure 8c). This Walker-type circulation transports moist air from the Pacific Ocean toward our target area through stronger zonal winds, supporting the findings presented by Limbu and Guirong (2019). The results also suggest that convergence activities across the domain are modulating the recent increase in EWDs.

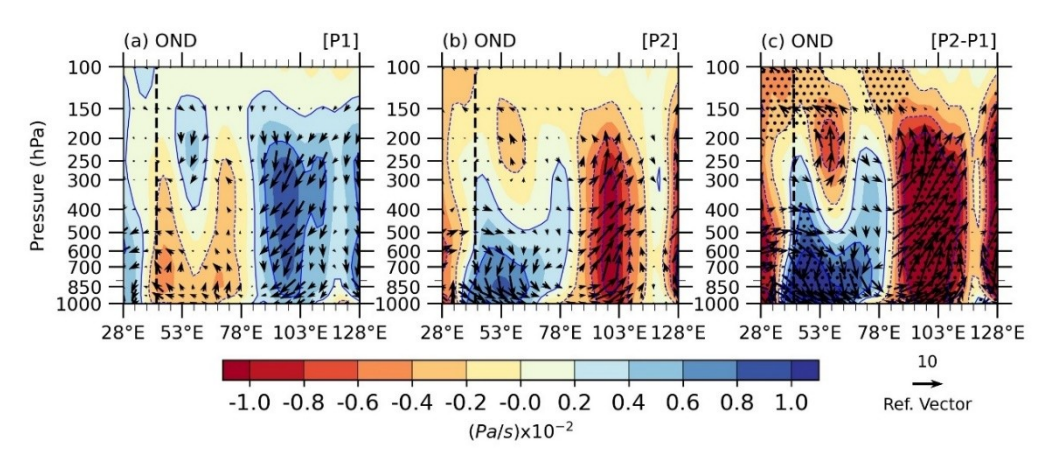


Figure 9: Vertical cross-section of zonal winds (unit: ms^{-1}) and vertical velocity (unit: $10^{-2} x Pas^{-1}$, shaded region) anomalies averaged along (0° to 12° S) during OND. (a) First period (1981-2010), (b) second period (2011-2020) and (c) Difference between periods. Stippling indicates a significant area at a 95% confidence level based on the Student t-test. The left side of the dotted vertical line (20°-42° E) shows the location of Tanzania.

Sea surface temperature anomalies and their relationship to the extreme wettest days

SST is one of the factors influencing the atmospheric circulations, variation of impacting moisture flux and convergence activities through teleconnection mechanisms. Therefore, tropical SSTs from 40° N to 60° S were analysed. The results generally show negative anomalies in the first period from 1981 to 2009 (Figure 9a) shifting to positive anomalies in the second period from 2010 to 2020 (Figure 9b), except for the central to eastern Pacific Ocean and same areas over the southwestern Atlantic Ocean (SWAO), performing oppositely. However, SST anomalies are generally increasing in the second period over the TIO and some parts of the Atlantic and Pacific Ocean during MAM, which concurs with the findings of Makula and Zhou (2021), found that in recent decades, tropical SST has been shifting from the cold phase to the warm phase. This shift of the SST from a cold phase to a warm phase, particularly over the TIO, probably enhanced radiative feedback atmosphere by adding warm-moist air. resulting in the recent increase of EWDs in the target domain.

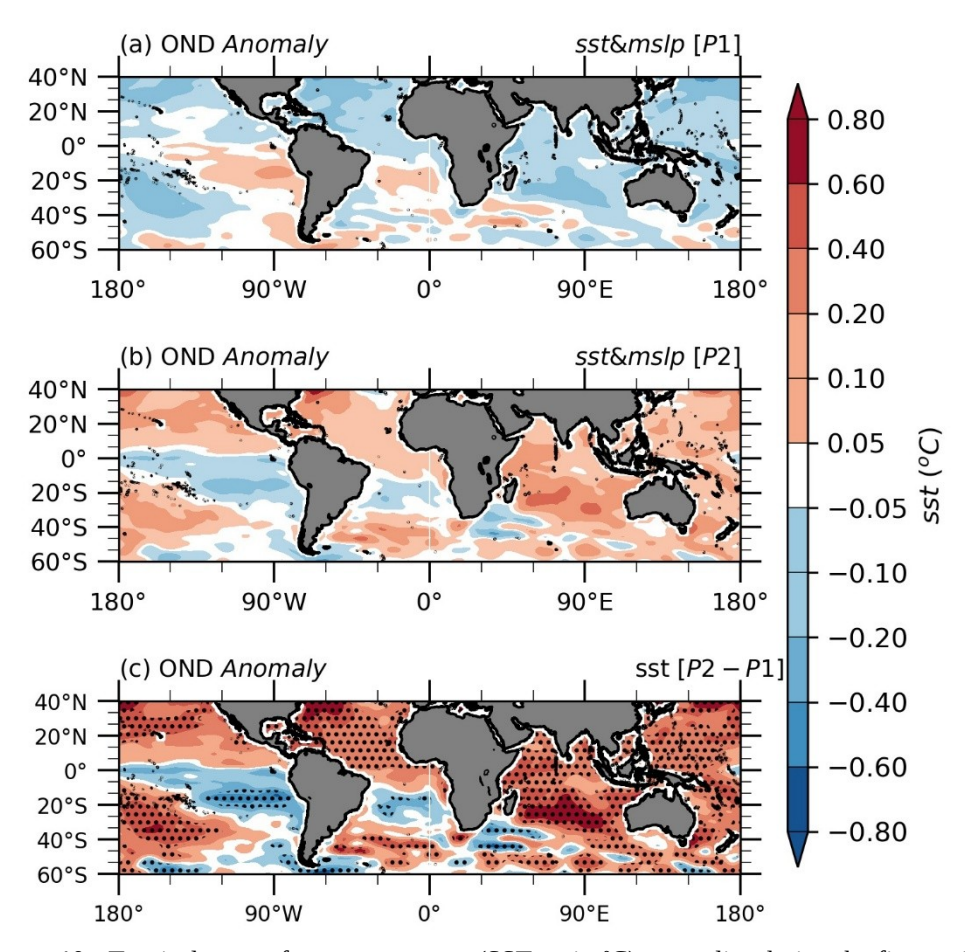


Figure 10: Tropical sea surface temperatures (SST, unit: ${}^{\circ}$ C) anomalies during the first period (a) and second period (b) and their differences (c). Stippling indicates a significant area at a 95% confidence level based on the *t*-test.

Coupled patterns between EWDs and SSTs

As we have seen in the previous subchapter, tropical SST anomalies generally shifted from a cold phase (in the first period) to the warm phase (in the second period). Therefore, this present study also examines the coupling between EWDs and SST over the Indian, Pacific, and Atlantic Oceans during OND. The first leading mode (SVD1) is explored during periods, as highlighted in Table 1. The results (Figure 10b and e) show warmer SST over most areas of the north and western Indian Ocean during the first and the second period, except in the tropical and southeastern Indian Ocean SWIO, showing cooling anomalies. These SSTs are accompanied by positive loading EWD anomalies, mostly in the bimodal region (Figure 10a) and extended southward in the second period (Figure 10d). Generally, results from SVD1 show that vast areas in bimodal regions are characterised by significant coupled patterns of positive EWD with much extent during the second period. This suggests that warming SSTs observed in the second period over the TIO substantially influence recently observed EWD Tanzania. These results are also in line with those of Kavishe and Limbu (2020) and Ongito and Limbu (2024) findings, which showed that warming SST anomalies over TIO are strongly linked to heavy rains in Tanzania, especially during the OND season.

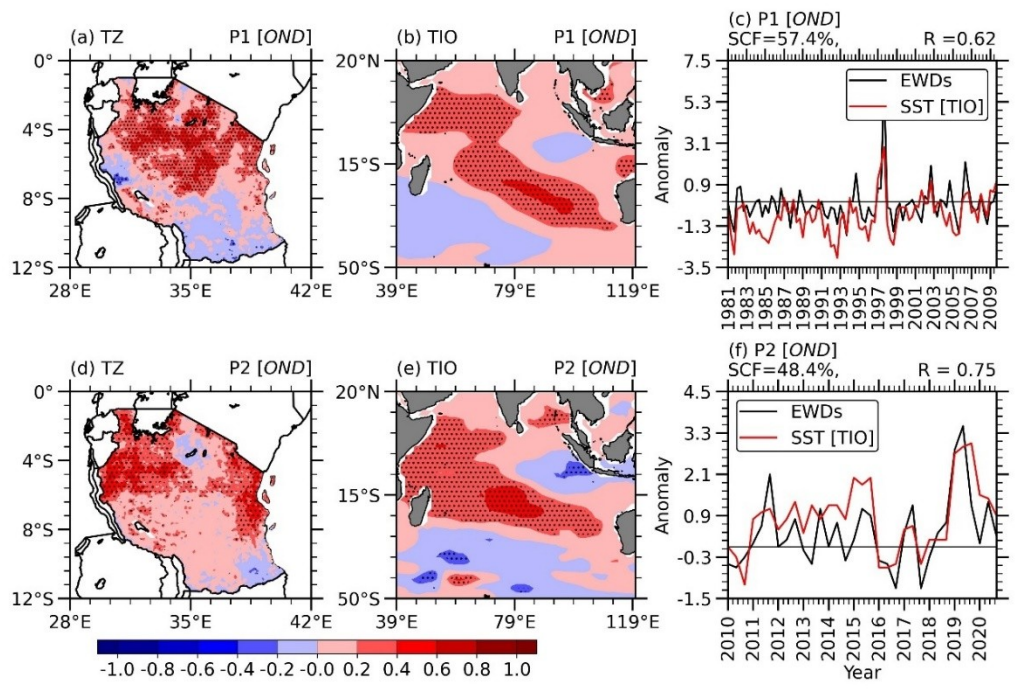


Figure 11: The first leading mode (SVD1) of the monthly Tropical Indian Ocean SSTs (39°–119°E and 20°N–50°S) and EWDs in Tanzania, during OND. First period (1981–2009) for: (a) EWDs, (b) SSTs and (c) Temporal patterns and linear correlation. Second period (2010-2020) for: (d) EWDs, (e) SSTs and (f) Temporal patterns and linear correlation. The black solid line corresponds to the expansion coefficient for EWDs, while the red solid line is for the SST anomaly. The correlation coefficients and square fraction coefficient of covariance are presented as R and SCF, respectively. Stippling indicates a significant area at a 95% confidence level based on the t-test.

Further analysis of the coupling between EWDs and SSTs over the Pacific Ocean was also conducted. The result shows that during the first period from 1981 to 2009 (Figure 11b), significant patterns at the 95% confidence level of warm SST are located over the tropical Pacific Ocean around the Niño3 regions between 60° E and 120° W, which stretched southeast to the northeast and formed like a triangle shape similar to El Niño Modoki (Ashok et al. 2007), however, warming much extended northeastern during the second period from 2010 to 2020 (Figure 11e). These patterns are generally coupled with positive loading of EWD over the

bimodal regions (Figure 11a and d). In summary, the SVD1 result shows warming SST over the tropical Pacific Ocean, which is characterised by an El Niño Modoki-like pattern that extends further northeast in the second period. These patterns are closely connected with the positive loading of EWD in the second period. The finding supports the previous studies by Preethi et al. (2015) and Ratnam et al. (2014), suggesting that El Niño Modoki significantly enhances rainfall in EA and reduces rainfall in the Sahel region and parts of the southern portion of Africa, below Tanzania.

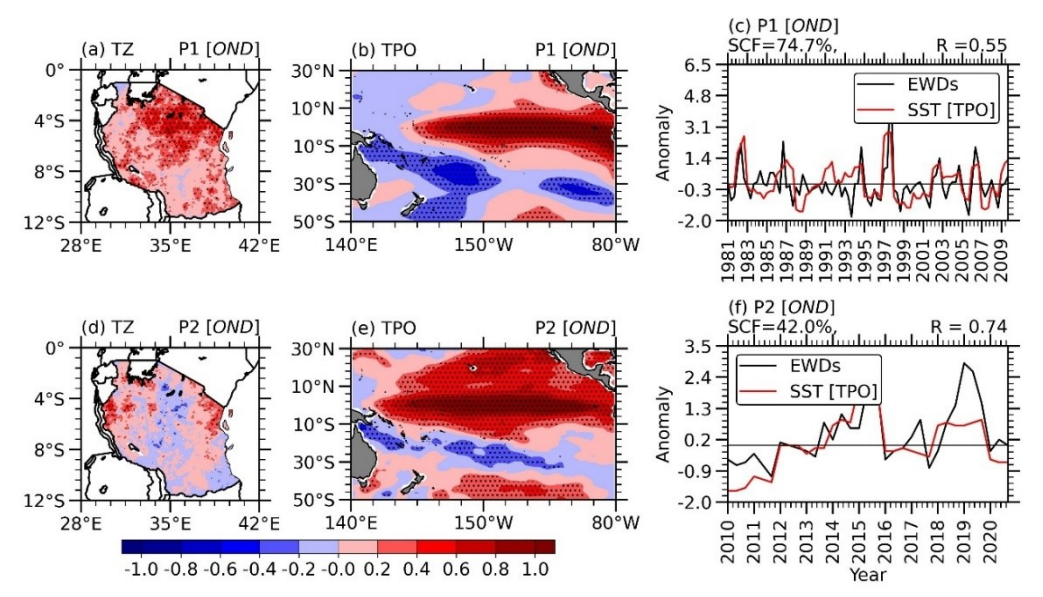


Figure 12: As in Figure 10, but for the tropical Pacific Ocean SSTs (80° W-140° E and 30° N-50° S).

Figure 11(b) demonstrates SST anomaly during the first period (1981-2009) with significant warming SST patterns at a 95% confidence level aroundt 0°-30° S, crossing east to west, while the remaining parts are characterised by cooling SSTs, which are coupled with positive loading anomalies over vast areas of Tanzania, especially western and central to north areas (Figure 11a). However, positive loading EWD patterns are shifted to northwestern, with a slight decrease in the eastern coast, central and NEH (Figure 11d) during the second period (2010-2020) which are strongly connected with warming SST between 5° N and 30° S and lower SSTs along 30°-40° S and 5°-15° N (Figure 11e). Generally, warming SST near the equator that extends northward and lower SST in the south are closely linked to positive loading EWDs, particularly during the second period, aligning with the findings of Limbu and Guirong (2019), indicating that warm (cool) SST anomalies in the southern Atlantic Ocean are associated with a decrease (increase) in rainfall over Tanzania during the OND seasons.

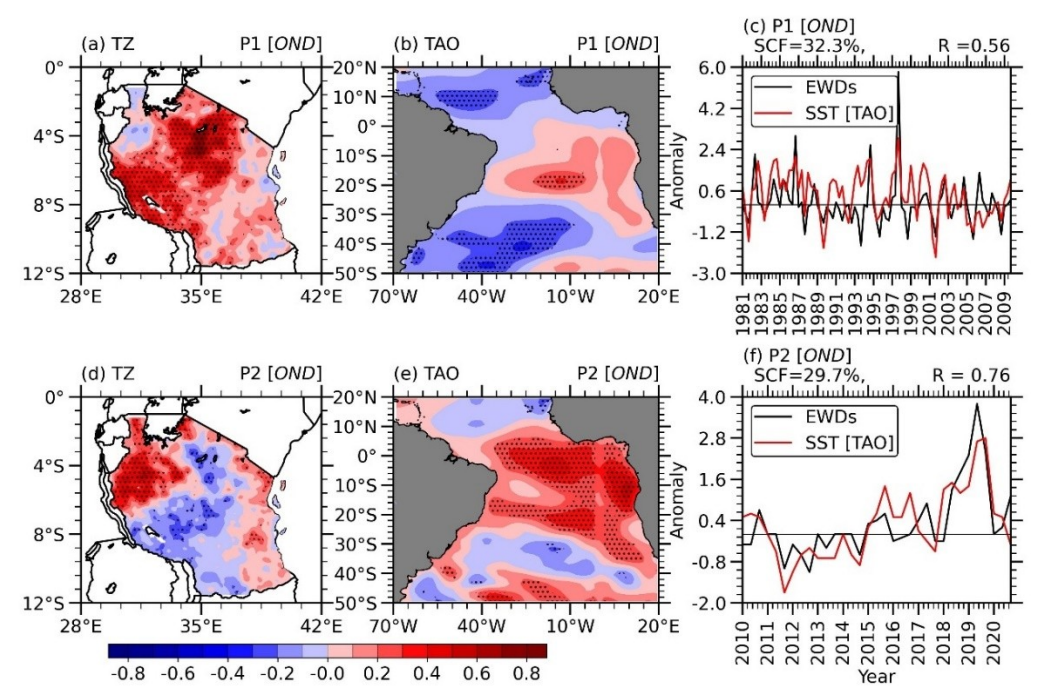


Figure 13: As in Figure 10, but for the tropical Atlantic Ocean SSTs (70° W-20° E and 20° N-50° S).

Furthermore, a linear relationship shows coupling patterns between Indian Ocean SST and EWDs during the first period (Figure 10c) with interannual patterns. The maximum positive amplitude occurred in 1997. In contrast, the second period shows dominant patterns of interannual oscillations with maximum amplitude in 2019 (Figure 10f). Moreover, similar patterns are depicted in Figure 11 (c and f), showing similar amplitudes in the same years. Linear timeseries of the Atlantic Ocean SSTs and EWDs (Figure 12c and f) show interannual oscillations, with the maximum positive amplitude of coupled anomalies occurring in 1997, which was the wettest year, and the minimum amplitude occurring in between 2001 and 2002, which were among the driest years in Tanzania, concur with results Chang'a observed et al. Additionally, most of the years with high amplitudes were associated with a positive peak of IOD and El Niño episodes, which are also linked with heavy rainfall events over the domain. This has also been manifested by Kavishe and Limbu. (2020), as well as Wainwright et al. (2020), who documented that pIOD and El Niño in 1997 and 2020 were strongly connected with an exceptional increase in rainfall over the EA.

On the other hand, statistical results from the SVD1 in the first and second periods are shown in Table 2, illustrating that the TIO and EWDs are linked more strongly in the second period, with the highest correlation (R \cong 0.75) and coupling SCF of about 57.4% in the first period. For the Pacific Ocean, the SSTs and EWDs account for 74.7% of the maximum SCF in the first period from 1981 to 2009, with their dominant coupled modes, characterised by a stronger correlation coefficient (R \cong 0.74) in the second period from 2010 to 2020. Atlantic Ocean SSTs and EWDs are characterised by less compared to other Oceans, with maximum correlation (R \approx 0.76) in the second period. These results suggest that tropical SSTs in the second period are among the factors that might contribute to the recent increase in EWDs in Tanzania, which also agrees with the results in Figure 9.

Table 2: Statistical summary of the SVD1 of squared covariance fraction (SCF) and linear correlation (R) between EWDs over Tanzania and SST over the tropical Indian, Pacific and Atlantic Oceans.

SVD1	Season	Indian Ocean		Pacific Ocean		Atlantic Ocean	
		1 st period	2 nd period	1 st period	2 nd period	1 st period	2 nd period
R	OND	0.62	0.75	0.55	0.74	0.56	0.76
SFC	OND	57.4%	48.4%	74.7%	42.0%	32.3%	27.7%

Note: All correlation values (R) are significant at the 99% confidence level based on the *t*-test.

Summary and Conclusion

This study explored the changes in EWDs in Tanzania and associated atmospheric and oceanic anomalies from 1981 to 2020. The study focuses on the OND rainfall season, which is commonly used for farming activities in Tanzania (Camberlin Philippon 2002, Hastenrath 2007). The result reveals EWDs patterns over the southwestern and parts of the eastern coast, LVB, as well as NEH regions. Trends show a significant increase in EWDs in the southwest of the LVB, and a non-significant decrease is observed over the northern part of Lake Victoria around the Simiyu region. The coverage of negative trend patterns is much experienced across central and extended to the south and SWH, which are significantly decreased at the 95% confidence level. Results from the time series showed an abrupt change in the trend of EWDs in 2010, which generally the pattern in time series indicates that years with a substantial number of EWDs, such as 1997 and 2019, are often linked to El Niño and pIOD events. This implies that El Niño and pIOD events are likely among the factors influencing the recent increase in EWDs in Tanzania.

Further analysis also indicates that the recent increase in EWDs is associated with abundant tropospheric moisture convergence (VIMFC) anomalies over the TIO, which extends to nearly the western side of the domain. The OND season is characterised by southeasterly VIMF vectors over the Indian Ocean, which then in turn eastward over the domain. enhancing rainfall formation. Overall, the recent period (2010-2020) has experienced a reduction in VIMF over a domain with a change in wind vector direction from easterly to westerly flow. Increasing evaporation was also observed over the Indian Ocean, Congo basin and some parts of the country in the second period, which supports the recent increase in EWDs. Moreover, the low-level trough with the ascending limb of Walker-type circulation over the WIO in the second period implies that convergence might be a dominant feature that enhances EWDs over the domain. Furthermore, shifting tropical SST from a cold phase in the first period (981-2009) to a warm phase in the second period (2010-2020), especially in TIO, also plays a great role in the recent increase of EWDs. The contribution of SSTs is also explicitly seen in SVD1, where the tropical Indian, Pacific and Atlantic Oceans are strongly coupled by EWDs during the second period with R=0.75, R=0.74 and R=0.76, respectively, which suggests that SST plays a substantial role in the recent increase in EWDs in Tanzania. Hence, the findings of this study provide valuable insights to farmers, water users and seasonal forecasters.

Declaration of interest

The authors declare no conflict of interest

References

Acharya N, Faniriantsoa R, Rashid B, Sultana R, Montes C and Dinku T 2020 Developing High-resolution Gridded Rainfall and Temperature Data for Bangladesh: the ENACTS-BMD dataset. Preprints. https://doi.org/10.20944/preprints202012.046 8.v1

Alexander LV, Zhang X, Peterson TC, Caesar J, Gleason B, Klein Tank AMG, Haylock M, Collins D, Trewin B, Rahimzadeh F, Tagipour A, Rupa Kumar K, Revadekar J, Griffiths G, Vincent L, Stephenson DB, Burn J, Aguilar E, Brunet M and Vazquez-Aguirre JL 2006 Global observed changes in daily climate extremes of temperature and precipitation. *J. Geophys. Res. Atmos.* 111(5): 1–22. https://doi.org/10.1029/2005JD006290

Anyamba A, Small JL, Britch SC, Tucker CJ, Pak EW, Reynolds CA, Crutchfield J and Linthicum KJ 2014 Recent weather extremes and impacts on agricultural production and vector-borne disease outbreak patterns. PLoS ONE 9(3): 23–24. https://doi.org/10.1371/journal.pone.0092538

Ashok K, Behera SK, Rao SA, Weng H and Yamagata T 2007 El Niño Modoki and its possible teleconnection. *J. Geophys. Res. Oceans* 112(11):

https://doi.org/10.1029/2006JC003798

Ashok K, Guan Z and Yamagata T 2001 Impact of the Indian Ocean dipole on the relationship between the Indian monsoon rainfall and ENSO. *Geophys. Res. Lett.* 28(23): 4499–4502.

https://doi.org/10.1029/2001GL013294

Awange JL, Saleem A, Sukhadiya RM, Ouma YO and Kexiang H 2019 Physical dynamics of Lake Victoria over the past 34 years (1984–2018): Is the lake dying? *Sci. Total Environ*. 658: 199–218. https://doi.org/10.1016/j.scitotenv.2018.12.051

Black E, Slingo J and Sperber KR 2003 An Observational Study of the Relationship between Excessively Strong Short Rains in Coastal East Africa and Indian Ocean SST. *Mon. Weather Rev.* 131(1): 74–94.

https://doi.org/10.1175/1520-

0493(2003)131<0074:AOSOTR>2.0.CO;2

Borhara K, Pokharel B, Bean B, Deng L and Wang SYS 2020 On Tanzania's precipitation climatology, variability, and future projection. *Climate* 8(2): 7–9.

https://doi.org/10.3390/cli8020034

Camberlin P, Moron V, Okoola R, Philippon N and Gitau W 2009 Components of rainy seasons' variability in Equatorial East Africa: Onset, cessation, rainfall frequency and intensity. *Theor. Appl. Climatol.* 98(3–4): 237–249.

https://doi.org/10.1007/s00704-009-0113-1 Camberlin P and Philippon N 2002 The East African March–May Rainy Season: Associated Atmospheric Dynamics and Predictability over the 1968–97 Period. *J.* Climate 15(9): 1002-1019.

https://doi.org/10.1175/1520-

0442(2002)015<1002:TEAMMR>2.0.CO;2 Chang'a LB, Kijazi AL, Luhunga PM, Ng'ongolo HK and Mtongor HI 2017 Spatial and Temporal Analysis of Rainfall and Temperature Extreme Indices in

Tanzania. *Atmos. Climate Sci.* 07(04): 525–539.

https://doi.org/10.4236/acs.2017.74038

Chang'a LB, Kijazi AL, Mafuru KB, Nying'uro PA, Ssemujju M, Deus B, Kondowe AL, Yonah IB, Ngwali M, Kisama SY, Aimable G, Sebaziga JN and Mukamana B 2020 Understanding the Evolution and Socio-Economic Impacts of the Extreme Rainfall Events in March-May 2017 to 2020 in East Africa. *Atmos. Climate Sci.* 10(04): 553–572.

https://doi.org/10.4236/acs.2020.104029

Chang'a L, Kijazi A, Mafuru K, Kondowe A, Osima S, Mtongori H, Ng'ongolo H, Juma O and Michael E 2020 Assessment of the Evolution and Socio-Economic Impacts of Extreme Rainfall Events in October 2019 over the East Africa. *Atmos. Climate Sci.* 10(03): 319–338.

https://doi.org/10.4236/acs.2020.103018

Chansaengkrachang K, Luadsong A and Aschariyaphotha N 2018 Vertically integrated moisture flux convergence over southeast Asia and its relation to rainfall over Thailand. *Pertanika J. Sci. Technol.* 26(1): 235–246.

Clark CO, Webster PJ and Cole JE 2003 Interdecadal Variability of the Relationship between the Indian Ocean Zonal Mode and East African Coastal Rainfall Anomalies. *J. Climate* 16(3): 548–554.

https://doi.org/10.1175/1520-

0442(2003)016<0548:IVOTRB>2.0.CO;2

Conway D 2002 Extreme Rainfall Events and Lake Level Changes in East Africa: Recent Events and Historical Precedents. 63–92. https://doi.org/10.1007/0-306-48201-0_2

Dinku T, Faniriantsoa R, Islam S, Nsengiyumva G and Grossi A 2022 The Climate Data Tool: Enhancing Climate Services Across Africa. *Front. Climate* 3(February): 1–16.

https://doi.org/10.3389/fclim.2021.787519

Dinku T, Funk C, Peterson P, Maidment R, Tadesse T, Gadain H and Ceccato P 2018 Validation of the CHIRPS satellite rainfall estimates over eastern Africa. *Q. J. R. Meteorol. Soc.* 144(August): 292–312. https://doi.org/10.1002/qj.3244

Dinku T, Ruiz F, Connor SJ and Ceccato P 2010 Validation and intercomparison of satellite rainfall estimates over Colombia. *J. Appl. Meteorol. Climatol.* 49(5): 1004–1014.

https://doi.org/10.1175/2009JAMC2260.1

Fasullo J and Webster PJ 2003 A hydrological definition of Indian Monsoon onset and withdrawal. *J. Climate* 16(19): 3200–3211. https://doi.org/10.1175/1520-0442(2003)016

<3200a:AHDOIM>2.0.CO;2

Finney DL, Marsham JH, Walker DP, Birch CE, Woodhams BJ, Jackson LS and Hardy S 2019 The effect of westerlies on East African rainfall and the associated role of tropical cyclones and the Madden–Julian Oscillation. *Q. J. R. Meteorol. Soc.* 146(727): 647–664.

https://doi.org/10.1002/qj.3698

Funk CC, Peterson PJ, Landsfeld MF, Pedreros DH, Verdin JP, Rowland JD, Romero BE, Husak GJ, Michaelsen JC and Verdin AP 2014 A Quasi-Global Precipitation Time Series for Drought Monitoring. *USGS Data Series* 832: 4.

Funk C, Peterson P, Landsfeld M, Pedreros D, Verdin J, Shukla S, Husak G, Rowland J. Harrison L, Hoell A and Michaelsen J The 2015 climate hazards infrared precipitation with stations -Α new environmental record for monitoring extremes. Sci. Data 2:

https://doi.org/10.1038/sdata.2015.66

Gamoyo M, Reason C and Obura D 2014 Rainfall variability over the East African coast. *Theor. Appl. Climatol.* 120(1): 311–322. https://doi.org/10.1007/s00704-014-1171-6

Han J, Miao C, Duan Q, Wu J, Gou J and Zheng H 2021 Changes in Unevenness of Wet-Day Precipitation Over China During 1961–2020. *J. Geophys. Res. Atmos.* 126(19): 1–18.

https://doi.org/10.1029/2020JD034483

Hastenrath S 2007 Circulation mechanisms of climate anomalies in East Africa and the equatorial Indian Ocean. *Dyn. Atmos. Oceans* 43(1–2): 25–35.

https://doi.org/10.1016/ j.dynatmoce.2006.06.002

Hersbach H, Bell B, Berrisford P, Hirahara S, Horányi A, Muñoz-Sabater J, Nicolas J, Peubey C, Radu R, Schepers D, Simmons A, Soci C, Abdalla S, Abellan X, Balsamo G, Bechtold P, Biavati G, Bidlot J, Bonavita M and Thépaut JN 2020 The ERA5 global reanalysis. *Q. J. R. Meteorol. Soc.* 146(730): 1999–2049.

https://doi.org/10.1002/qj.3803

IPCC 2012 Managing the Risks of Extreme Events and Disasters to Advance Climate Change Adaptation. *IPCC Special Report*. https://doi.org/10.1017/CBO978113917724 5.009

Indeje M and Semazzi FHM 2000 ENSO signals in East African Rainfall seasons. *Int. J. Climatol.* 20: 19–46.

https://doi.org/10.1002/(SICI)1097-0088(200001)20:1<19::AID-JOC449>3.0.CO;2-0

Ishii M, Shouji A, Sugimoto S and Matsumoto T 2005 Objective analyses of sea-surface temperature and marine meteorological variables for the 20th century using ICOADS and the Kobe Collection. *Int. J. Climatol.* 25(7): 865–879. https://doi.org/10.1002/joc.1169

Japheth LP, Tan G, Chang'a LB, Kijazi AL, Mafuru KB and Yonah I 2021 Assessing the Variability of Heavy Rainfall during October to December Rainfall Season in Tanzania. *Atmos. Climate Sci.* 11(02): . https://doi.org/10.4236/acs.2021.112016

Kalnay E, Kanamitsu M, Kistler R, Collins W, Deaven D, Gandin L, Iredell M, Saha S, White G, Woollen J, Zhu Y, Chelliah M, Ebisuzaki W, Higgins W, Janowiak J, Mo KC, Ropelewski C, Wang J, Leetmaa A and Joseph D 1996 The NCEP/NCAR 40-Year Reanalysis Project. *Bull. Am. Meteorol. Soc.* 77(3): 437–472.

https://doi.org/10.1175/1520-

0477(1996)077<0437:TNYRP>2.0.CO;2 Kavishe GM and Limbu PTS 2020 Variation of October to December rainfall in Tanzania and its association with sea surface temperature. *Arab. J. Geosci.* 13(13): https://doi.org/10.1007/s12517-020-05535-z

Kebacho LL 2022a Interannual variations of the monthly rainfall anomalies over Tanzania from March to May and their associated atmospheric circulations anomalies. *Nat. Hazards* 112(1): 163–186. https://doi.org/10.1007/s11069-021-05176-9

Kebacho LL 2022b The Role of Tropical Cyclones Idai and Kenneth in Modulating Rainfall Performance of 2019 Long Rains over East Africa. *Pure Appl. Geophys.* 179(4): 1387–1401.

https://doi.org/10.1007/s00024-022-02993-2

Kendall MG 1975 Rank correlation methods. *Griffin, London.*

Kijazi AL and Reason CJC 2009 Analysis of the 2006 floods over northern Tanzania. *Int. J. Climatol.* 29(7): 955–970.

https://doi.org/10.1002/joc.1846

Kijazi AL and Reason CJC 2011 Intraseasonal variability over the northeastern highlands of Tanzania. *Int. J. Climatol.* 32(6): 874–887.

https://doi.org/10.1002/joc.2315

Kilavi M, MacLeod D, Ambani M, Robbins J, Dankers R, Graham R, Helen T, Salih AAM and Todd MC 2018 Extreme rainfall and flooding over Central Kenya Including Nairobi City during the long-rains season 2018: Causes, predictability, and potential for early warning and actions. *Atmosphere* 9(12):

https://doi.org/10.3390/atmos9120472

Kotz M, Levermann A and Wenz L 2022 The effect of rainfall changes on economic production. *Nature* 601(7892): 223–227. https://doi.org/10.1038/s41586-021-04283-8 Li J and Wang B 2018 Predictability of summer extreme precipitation days over eastern China. *Clim. Dyn.* 51(11–12): 4543–4554. https://doi.org/10.1007/s00382-017-3848-x

Li X, Zhou W, Li C and Song J 2013 Comparison of the annual cycles of moisture supply over Southwest and Southeast China. *J. Climate* 26(24): 10139–10158.

https://doi.org/10.1175/JCLI-D-13-00057.1

Limbu PTS and Guirong T 2019 Relationship between the October-December rainfall in Tanzania and the Walker circulation cell over the Indian Ocean. *Meteorol. Z.* 28(6): 453–469.

https://doi.org/10.1127/metz/2019/0939

Limbu PTS and Guirong T 2020 Influence of the tropical Atlantic Ocean and its Walker circulation cell on October–December rainfall variability over Tanzania. *Int. J. Climatol.* 40(13): 5767–5782.

https://doi.org/10.1002/joc.6550

Lyon B and DeWitt DG 2012 A recent and abrupt decline in the East African long rains. *Geophys. Res. Lett.* 39(2): 1–5. https://doi.org/10.1029/2011GL050337

Ma J, Ju Q, Du Y, Liu Y, Wang G, Zeng H and Hao Z 2022 Assessing precipitation variations in the Yangtze River Basin during 1979–2019 by vertically integrated moisture flux divergence. *Nat. Hazards* 114(1): 971–987.

https://doi.org/10.1007/s11069-022-05419-3

Mafuru KB and Guirong T 2020 Causes of the upper-level warm temperature anomaly (UWTA) associated with March–May heavy rainfall in Tanzania. *Atmos. Res.* 242(April): 105016.

https://doi.org/10.1016/j.atmosres.2020.105016
Makula EK, Umutoni MA, Japheth LP,
Lipiki EJ, Kebacho LL and Limbu PTS
2020 The Covariability of Sea Surface
Temperature and MAM Rainfall on East
Africa Using Singular Value
Decomposition Analysis. Geogr.
Pannonica 24(4): 261–270.

https://doi.org/10.5937/GP24-27577

Makula EK and Zhou B 2021 Changes in March to May rainfall over Tanzania during 1978–2017. *Int. J. Climatol.* 41(12): 5663–5675. https://doi.org/10.1002/joc.7146 Mann HB 1945 Nonparametric Tests Against Trend. *Econometrica* 13(3): 245. https://doi.org/10.2307/1907187

Mastrantonas N, Herrera-Lormendez P, Magnusson L, Pappenberger F and Matschullat J 2020 Extreme precipitation events in the Mediterranean: Spatiotemporal characteristics and connection to large-scale atmospheric flow patterns. *Int. J. Climatol.* 41(4): 2710–2728.

https://doi.org/10.1002/joc.6985

Mbigi D and Xiao Z 2021 Tanzanian rainfall responses to El Niño and positive Indian Ocean Dipole events during 1951–2015. *Atmos. Oceanic Sci. Lett.* 14(6): 100093.

https://doi.org/10.1016/j.aosl.2021.100093

Mtewele ZF, Xu X and Jia G 2021 Heterogeneous Trends of Precipitation Extremes in Recent Two Decades over East Africa. *J. Meteorol. Res.* 35(6): 1057–1073. https://doi.org/10.1007/s13351-021-1028-8

Mugalavai EM, Kipkorir EC, Raes D and Rao MS 2008 Analysis of rainfall onset, cessation and length of growing season for western Kenya. *Agric. For. Meteorol.* 148(6): 1123–1135.

https://doi.org/10.1016/j.agrformet.2008.02.013 Nairobi NS 1979 The East African monsoons

and their effects on agriculture. *GeoJournal* 3(2): 193–200.

https://doi.org/10.1007/BF00257708

Nandargi S and Mulye SS 2012 Relationships between rainy days, mean daily intensity, and seasonal rainfall over the Koyna catchment during 1961–2005. *Sci. World J.* 2012:

https://doi.org/10.1100/2012/894313

Ndabagenga DM, Yu J, Mbawala JR, Ntigwaza CY and Juma AS 2023 Climatic Indices' Analysis on Extreme Precipitation for Tanzania Synoptic Stations. *J. Geosci. Environ. Prot.* 11(12): 182–208. https://doi.org/10.4236/gep.2023.1112010

Ntwali D, Ogwang BA and Ongoma V 2016 The Impacts of Topography on Spatial and Temporal Rainfall Distribution over Rwanda Based on WRF Model. *Atmos. Climate Sci.* 06(02): 145–157. https://doi.org/10.4236/acs.2016.62013

Nyamweya C, Lawrence TJ, Ajode MZ, Smith S, Achieng AO, Barasa JE, Masese FO, Taabu-Munyaho A, Mahongo S, Kayanda R, Rukunya E, Kisaka L, Manyala J, Medard M, Otoung S, Mrosso H, Sekadende B, Walakira J, Mbabazi S and Nkalubo W 2023 Lake Victoria: Overview of research needs and the way forward. *J. Great Lakes Res.* 49(6): 102211. https://doi.org/10.1016/j.jglr.2023.06.009

Ogwang BA, Haishan C and Guirong T 2012 Diagnosis of September - November Drought and the Associated Circulation Anomalies Over Uganda. *Pak. J. Meteorol.* 9(17): 11–24.

Ojara MA, Yunsheng L, Babaousmail H and Wasswa P 2021 Trends and zonal variability of extreme rainfall events over East Africa during 1960–2017. *Nat. Hazards* 109(1): 33–61.

https://doi.org/10.1007/s11069-021-04824-4

Omay PO, Muthama NJ, Oludhe C, Kinama JM, Artan G and Atheru Z 2023 Observed changes in wet days and dry spells over the IGAD region of eastern Africa. *Sci. Rep.* 13(1): https://doi.org/10.1038/s41598-023-44115-5

Ongito BW and Limbu PTS 2024 Quantifying the Strength of the El Niño Southern Oscillation and the Indian Ocean Dipole in Influencing the OND Rainfall Season in Tanzania. *Tanz. J. Sci.* 49(5): 1110–1126.

https://doi.org/10.4314/tjs.v49i5.14

Ongoma V, Chen H and Omony GW 2016 Variability of extreme weather events over the equatorial East Africa, a case study of rainfall in Kenya and Uganda. *Theor. Appl. Climatol.* 131(1–2): 295–308.

https://doi.org/10.1007/s00704-016-1973-9 Owiti Z 2012 Spatial distribution of rainfall seasonality over East Africa. *J. Geogr. Reg. Plann.* 5(15): 409–421.

https://doi.org/10.5897/jgrp12.027

Palmer PI, Wainwright CM, Dong B, Maidment RI, Wheeler KG, Gedney N, Hickman JE, Madani N, Folwell SS, Abdo G, Allan RP, Black ECL, Feng L, Gudoshava M, Haines K, Huntingford C, Kilavi M, Lunt MF, Shaaban A and Turner AG 2023 Drivers and impacts of Eastern African rainfall variability. *Nat. Rev. Earth Environ.* 4(4): 254–270.

https://doi.org/10.1038/s43017-023-00397-x Pettitt A 1979 A Non-parametric to the Approach Problem. *Appl. Stat.* 28(2): 126–135.

Preethi B, Sabin TP, Adedoyin JA and Ashok K 2015 Impacts of the ENSO Modoki and other tropical indo-pacific climate-drivers on African rainfall. *Sci. Rep.* 5: 1–15.

https://doi.org/10.1038/srep16653

Prohaska JT 1976 A Technique for

Analyzing the Linear Relationships between Two Meteorological Fields. *Mon. Weather Rev.* 104(11): 1345–1353.

https://doi.org/10.1175/1520-

0493(1976)104<1345:ATFATL>2.0.CO;2

Ratnam JV, Behera SK, Masumoto Y and Yamagata T 2014 Remote effects of El Niño and Modoki events on the austral summer precipitation of Southern Africa. *J. Climate* 27(10): 3802–3815. https://doi.org/10.1175/JCLI-D-13-00431.1

Rwambo I, Fan Y, Yu P, Chu C, Nyasulu M and King'uza P 2025 Interannual variability of short rains in Tanzania and the influences from ENSO and the Indian Ocean Dipole. *Atmos. Oceanic Sci. Lett.* 100614.

https://doi.org/10.1016/j.aosl.2025.100614
Saji NH and Yamagata T 2003 Possible impacts of Indian Ocean Dipole mode events on global climate. *Clim. Res.* 25(2): 151–169.

Semgomba DS, Deng J and King'uza PH 2025 Interannual Relationship between ENSO and Tropical Cyclone Genesis over the Southwest Indian Ocean and Its Modulation by the Interdecadal Pacific Oscillation. *J. Geosci. Environ. Prot.* 13(3): 29–46.

https://doi.org/10.4236/gep.2025.133002

Spracklen DV, Arnold SR and Taylor CM 2012 Observations of increased tropical rainfall preceded by air passage over forests. *Nature* 489: 282–285.

https://doi.org/10.1038/nature11390

Tadross M, Suarez P, Lotsch A, Hachigonta S, Mdoka M, Unganai L, Lucio F, Kamdonyo D and Muchinda M 2009 Growing-season rainfall and scenarios of future change in southeast Africa: Implications for cultivating maize. *Clim. Res.* 40(2–3): 147–161.

https://doi.org/10.3354/cr00821

Thornton PK, Ericksen PJ, Herrero M and Challinor AJ 2014 Climate variability and vulnerability to climate change: A review. *Glob. Change Biol.* 20(11): 3313–3328.

https://doi.org/10.1111/gcb.12581

USAID 2018 Climate Change in Tanzania: Country Risk Profile. https://www.climatelinks.org/sites/default/fi les/asset/document/Tunisia_CRP.pdf

Vellinga M and Milton SF 2018 Drivers of interannual variability of the East African "Long Rains". *Q. J. R. Meteorol. Soc.* 144(712): 861–876.

https://doi.org/10.1002/qj.3263

Verburg P and Hecky RE 2009 The physics of the warming of Lake Tanganyika by climate change. *Limnol. Oceanogr.* 54(6 PART 2): 2418–2430.

https://doi.org/10.4319/

lo.2009.54.6_part_2.2418

Wagesho N and Claire M 2016 Analysis of Rainfall Intensity-Duration-Frequency Relationship for Rwanda. *J. Water Resour. Prot.* June 2016: 706–723.

https://doi.org/10.4236/jwarp.2016.87058

Wainwright CM, Finney DL, Kilavi M, Black E and Marsham JH 2020 Extreme rainfall in East Africa, October 2019–January 2020 and context under future climate change. *Weather* 3(January): 1–6. https://doi.org/10.1002/wea.3824

Wang B, Zhang M, Wei J, Wang S, Li S, Ma Q, Li X and Pan S 2012 Changes in extreme events of temperature and precipitation over Xinjiang, northwest China, during 1960–2009. *Quat. Int.* 298: 141–151.

https://doi.org/10.1016/j.quaint.2012.09.01

Wang Y, Zhou B, Qin D, Wu J, Gao R and Song L 2017 Changes in mean and extreme temperature and precipitation over the arid region of northwestern China: Observation and projection. *Adv. Atmos. Sci.* 34(3): 289–305. https://doi.org/10.1007/s00376-016-6160-5

Wenhaji NC, Cattani E, Merino A and Levizzani V 2018 An observational study of the variability of East African rainfall with respect to sea surface temperature and soil moisture. *Q. J. R. Meteorol. Soc.* 144: 384–404. https://doi.org/10.1002/qj.3255

Wiston M and Mphale KM 2019 Mesoscale convective systems: A case scenario of the "heavy rainfall" event of 15–20 January 2013 over southern Africa. *Climate* 7(6): https://doi.org/10.3390/cli7060073

WMO 2023 Economic costs of weatherrelated disasters soars but early warnings save lives. https://www.meteorologicaltechnologyinter national.com/news/extreme-weather/cost-of-weather-related-disasters-soars-but-early-warnings-save-lives.html

Xie H, Li D and Xiong L 2014 Exploring the ability of the Pettitt method for detecting change point by Monte Carlo simulation. *Stoch. Environ. Res. Risk Assess.* 28(7): 1643–1655.

https://doi.org/10.1007/s00477-013-0814-y Yonah IB, King'uza PH, Chang'a LB, Babyegeye MM, Mahoo HF and Kijazi AL 2023 The Inter-Annual Variability of Rainfall Onset and Its Implication on Crop Planting in Selected East Africa Countries. *Am. J. Climate Change* 12(02): 268–291. https://doi.org/10.4236/ajcc.2023.122010 Zhang Q, Holmgren K and Sundqvist H 2015 Decadal rainfall dipole oscillation over Southern Africa modulated by variation of austral summer land-sea contrast along the east coast of Africa. *J. Atmos. Sci.* 72(5): 1827–1836. https://doi.org/10.1175/JAS-D-14-0079.1